Technical Report

Department of Computer Science
and Engineering
University of Minnesota
4-192 EECS Building
200 Union Street SE
Minneapolis, MN 55455-0159 USA

TR 05-032

Strategies for the Visualization of Multiple Co-located Vector Fields

Timothy Matthew Urness, Victoria Interrante, Ellen Longmire, Ivan Marusic, Sean O'neill, and Thomas W. Jones

September 22, 2005

Strategies for the Visualization of Multiple Co-located Vector Fields

Timothy Urness* **Victoria Interrante**
Department of Computer Science

Ellen Longmire **Ivan Marusic**
Department of Aerospace Engineering and Mechanics

Sean O'Neill **Thomas W. Jones**
Department of Astronomy

University of Minnesota

*e-mail: urness@cs.umn.edu

September 2005

Abstract

Fluids research often involves developing theories about the complex relationships between multiple scalar and vector quantities. We discuss strategies for effectively visualizing co-located vector fields, enabling the key physical structures of one vector field to be clearly understood within the context of a related vector field. We describe the range of effects that can be obtained by combining several existing flow visualization techniques for the purposes of analyzing multiple vector fields. Results are shown through two distinctly different scientific applications: the visualization of velocity and vorticity fields in experimentally acquired turbulent boundary layer flow data, and the visualization of velocity and magnetic fields in computational simulations of astrophysical jets.

1 Introduction

1.1 Experimental Turbulent Flow Visualization

The study of coherent structures in turbulent boundary layers is an active area of research. Driven by applications including the reduction of turbulent skin-friction drag over aircraft, researchers have long been interested in developing a deeper understanding of the key physical features within turbulent flows. Of particular interest is the analysis of multiple scalar and vector distributions and how the interaction of variables contribute to theories of drag and the formation of vortex packets within a turbulent boundary layer. This analysis remains limited mainly because of a lack of understanding of the complicated interactions that occur between the vortices that make up the motion.

Stereoscopic *particle image velocimetry* (PIV) is a technique that can be used to experimentally measure instantaneous components of a velocity field in a plane of a turbulent boundary layer in a moderate to high Reynolds number flow. In addition to the experimentally-generated velocity field ($\vec{v}$), the *vorticity* vector field ($\vec{w} = \nabla \times \vec{v}$) can be numerically calculated and analyzed with the velocity vector field. While this data is sampled on a 2D plane, the resulting footprint of the multi-variate data gives insight into the structure and behavior of the 3D flow. Because the process of knowledge discovery related to this application is predicated on the ability to achieve an integrated understanding of the individual contribution of each variable and of how the variables interrelate with each other, developing effective multi-variate visualization methods is of critical importance to facilitating the understanding and analysis of results from the PIV experiments.

1.2 Computational Physics Visualization

Current research conducted in the field of computational physics focuses on modeling 3D magnetohydrodynamic light supersonic jets in the context of astrophysical jets in galaxy clusters. These high-speed jets propagate distances of over 650,000 light years from their sources, transporting energy and magnetic fields to their surrounding environments. The jet magnetic field is advected along with the flow and is expected to reflect properties of the evolving velocity field. Of particular interest is the extent to which the magnetic field and velocity vector fields are spatially aligned and/or orthogonal to one another.

In addition to understanding the relationship of the topology of both vector fields, astrophysicists are interested in the interplay between magnetic field strength and the corresponding velocity structures as magnetic field enhancement naturally results from shear and compression in the flow.

Detailed studies of these issues help researchers to understand how kinetic and magnetic energy distributions evolve in these systems and provide insight into the relationships between flow structure and the magnetic fields associated with observed radio emission. We support this analysis by developing tools that allow the visualization of both fields simultaneously.

1.3 Multi-variate Visualization

The visualization of multiple co-located data fields can be done in several ways. One method is to display the individual distributions in a side-by-side manner, so that each field can be seen clearly and independently. However, spatial correspondences between distributions are not easily revealed using this technique. Another approach is to show multiple fields sequentially in the same space and allow the user to quickly alternate between the images. With this approach, however, it is difficult to obtain a reliable, *integrated* understanding of the multiple fields.

The goal of our research is to explore strategies for developing effective methods for the visual representation of multiple co-located vector and scalar fields to allow each field to be understood and analyzed both individually and in the context of the other. Mining the knowledge base of previous visualization research yields important findings and insight to assist the research of our specific applications. Using these insights, we are able to re-construct, manipulate, and expand upon the existing state-of-the-art in order to further the process of knowledge discovery related to specific tasks and conditions. Our present efforts focus primarily on the investigation of methods for effectively visualizing multiple fields defined over a 2D domain; the problem of effectively visualizing multiple fields defined over a 3D domain is even more challenging, and an important area for future work.

2 Classifying and Combining Visualization Techniques

2.1 Classification

We classify existing 2D vector field flow visualization techniques into one of three visually distinct categories: texture-based, line-based, or glyph-based.

Texture-based techniques are characterized by a consistent, highly-detailed, and dense representation of a vector field. Many texture-based techniques have been developed for the visualization of 2D flow as it allows for the fine details of a vector field to be easily displayed and analyzed. The pioneering technique of "Spot Noise" produces a texture from weighted and randomly positioned spots deformed in accordance with the direction of flow [11]. Line Integral Convolution (LIC), a widely-used technique, involves convolving a white noise input texture along calculated streamlines [1]. Ambiguous flow direction in LIC images can be resolved by animating the texture. Texture synthesis has also been used to depict a vector field [7].

Line-based techniques involve the display of elongated *streamlines* – segments that are everywhere tangent to the vector field. These images are fundamentally different than the images created with texture-based techniques as streamlines can be visually traced over a long distance, and line-based images are more sparse than textures. While streamlines give a global sense of flow by depicting paths along the vector field, flow direction is not always apparent. Additionally, locating an advantageous small number of critical lines representing the flow can be a challenging problem. Turk and Banks developed a technique for achieving an evenly spaced field of streamlines, based on the use of an energy function to guide the placement and growth of the lines [8].

Glyph-based techniques are characterized by the use of repeatable icons that can express various types of information about the flow, including flow orientation. The most basic technique is the use of hedgehogs (sometimes referred to as vector plots) – short line segments or arrows aligned with the flow direction at regularly or randomly distributed locations. Glyphs provide the ability to depict flow direction by using the glyph shape or a luminance ramp. We also include in this category techniques that involve placing glyphs along calculated streamlines.

2.2 Combining Multiple Images

Transparency or layering is one of the most effective methods to portray relationships between overlaying components. Kirby et al. introduced a method inspired by the layering techniques used in oil paintings to visualize components of 2D flow data [5]. Interrante has used transparent stroked textures on 3D surfaces superimposed over underling opaque structures [3]. Weigle et al. demonstrated a texture generation technique, based on the layering of oriented slivers,

using orientation and luminance to encode multiple overlapping scalar fields [12]. Hotz et al. vary the input texture density and spot size in addition to kernel length and overlay sparse LIC images to visualize features of a tensor field [2]. Our research is inspired by these techniques, and seeks to expand the applications of layering in the visualization of multiple related vector and scalar fields.

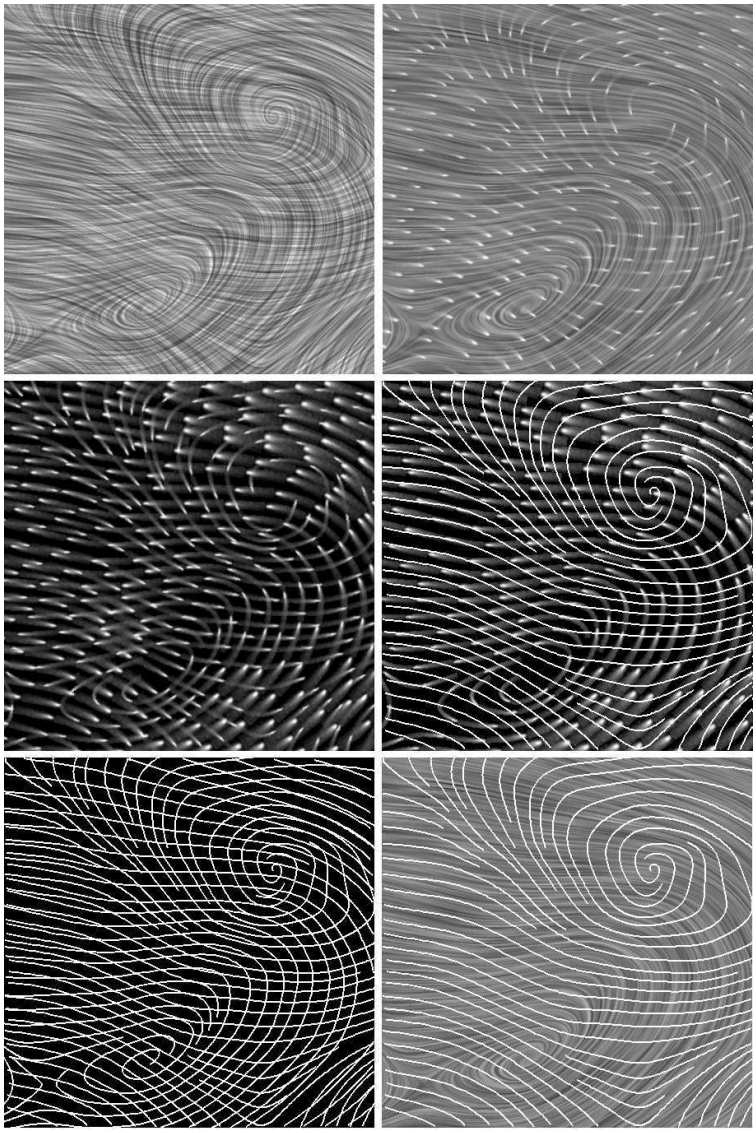

Figure 1: Different 2D vector visualization techniques applied to the visualization of two co-located vector fields.

3 Dual Vector Fields

Considering one sample from each of the three visually distinct methods for vector field visualization (texture, line and glyph) we explore the range of effects that can be achieved using layered combinations of these approaches to visualize two different, co-located vector fields (figure 1). For the texture-based sample, we use LIC – the most widely used texture-based approach. For the glyph-based sample, we create an image by repeatedly texture mapping a comet-like glyph along thick, equally spaced streamlines. This results in a sequence of glyphs that is continuous in the direction of the flow. The line-based sample is created using the source code supplied by the authors of the equally-spaced streamline technique [8].

One of the primary goals in each of the applications is to depict the key physical structures of one vector field in the context of the key physical structures in another. Therefore, it is highly desirable to be able to easily differentiate between the visual representations of each field and to easily identify each distribution. This process becomes more complicated when the same representational technique (e.g. line, texture or glyph) is applied to each field. While a supplemental visual variable, such as color, could be used to distinguish the two representations, we would ideally prefer to be able to reserve the use of color for the communication of related, co-located scalar quantities.

The problem of differentiating between each vector field is illustrated on the left hand side of figure 1. The combination of two texture-based techniques (upper left) provides a rich representation in which both vector fields are visible, particularly in regions where the vector field orientations are not aligned. However, it becomes challenging to distinguish the two datasets in regions where the orientations are aligned as it is difficult to determine which field is being represented by which texture at any given location. Both the glyph and line techniques utilize an inherently sparse streamline spacing that leaves empty space in the image. Combining two sparse techniques creates in a large amount of negative space which can result in a lost opportunity to represent fine details of the vector fields. When two glyph-based techniques are overlaid (center left image of figure 1), maintaining good visual continuity or "good continuation" in the direction of the flow in each field becomes a challenge, particularly when the glyphs are separated by a nontrivial amount of empty space. When two line-based techniques are overlaid (lower left image of figure 1), the continuity of streamlines is maintained; however, the accidental patterns of intersections between streamlines in different vector fields can lead to visual artifacts that may cause an inaccurate perception of the data (figure 2).

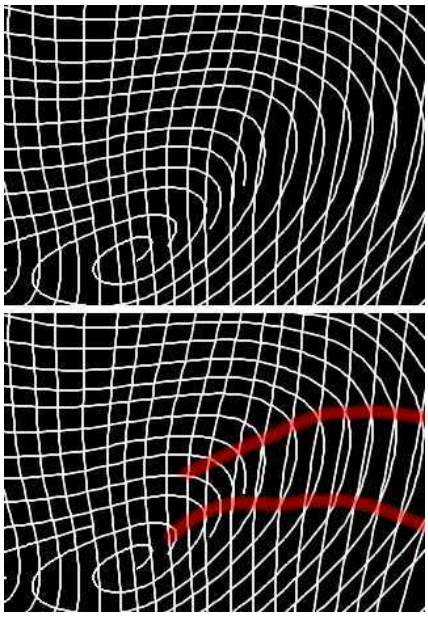

Figure 2: Combining streamline representations can lead to visual artifacts. Top: Two streamline images are combined. Bottom: the artifact caused by intersecting streamlines is highlighted

When a different representational approach is used for each field, the primary challenge is to appropriately balance the visual prominence of each representation, so that neither overwhelms the other in the combined presentation. Figure 3 illustrates how different representations can be made more or less prominent by altering the contrast and luminance values prior to layering the two images. Similarly, differences in line thickness can be used to make one vector field more prominent when displayed with another (figure 4).

In our experience, particularly good results can be achieved by layering a relatively sparser, higher contrast, glyph or line-based representation of one field over a relatively denser, lower contrast, texture-based representation of the other field. The high contrast between the glyph or line elements and the background or empty space enables them to maintain their visibility when superimposed over the textured background; the relatively sparse distribution of the glyph or line elements in the top-layer flow is necessary to enable the simultaneous, effortless appreciation of the flow that is portrayed on the underlying layer.

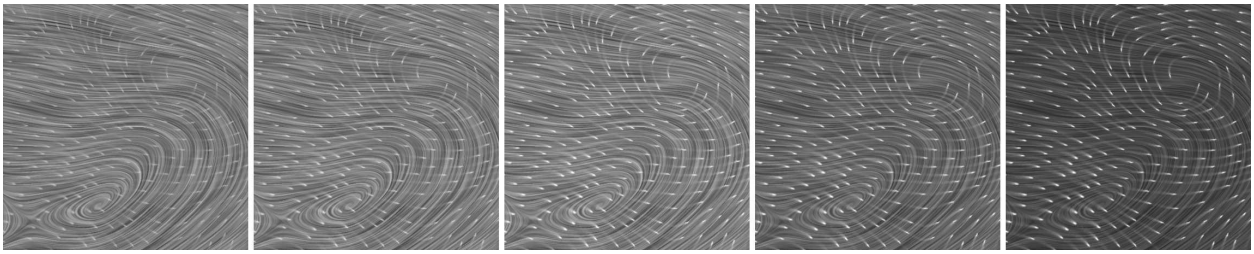

Figure 3: Different representations can be emphasized by altering luminance properties of individual representations prior to image compositing. In the sequence from left to right of images above, the glyphs become brighter while the texture becomes darker. When the glyphs are very subtle (left image), the vector field represented by the texture is more prominent. When the contrast between the white glyphs and the darkened texture is more obvious (right image), the vector field represented by the glyphs is more prominent.

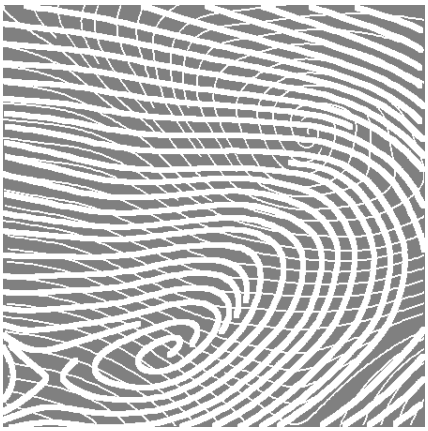

Figure 4: Differences in line thickness cause one vector field to appear more prominently than the other.

Next we illustrate methods that allow for two different representations to be combined in such a way that each representation remains distinct and visually separable.

3.1 Overlay

In figure 5, two representations are combined using a *screen overlay* method. This method is similar to a standard image multiplication operation but operates on the additive inverse of each input image. Specifically, if $D(x,y)$ is the output image and $A(x,y)$ and $B(x,y)$ are the respective input images, and we assume that each pixel intensity is between 0.0 and 1.0, the *screen overlay* operation is defined as

$$D(i,j) = 1.0 - (1.0 - A(i,j)) * (1.0 - B(i,j))$$

Applying this formula allows the intensities of the underlying texture image to show through in the places where the overlying glyph image contains empty (black) space. Of note in figure 5 is that the two vector fields can be easily distinguished not only where their orientations are nearly orthogonal, but also in the places (such as the upper right corner) where their orientations are nearly aligned. It is precisely to enable these sorts of comparisons of the relative alignments of the two fields that we pursue these investigations of methods for their combined portrayal.

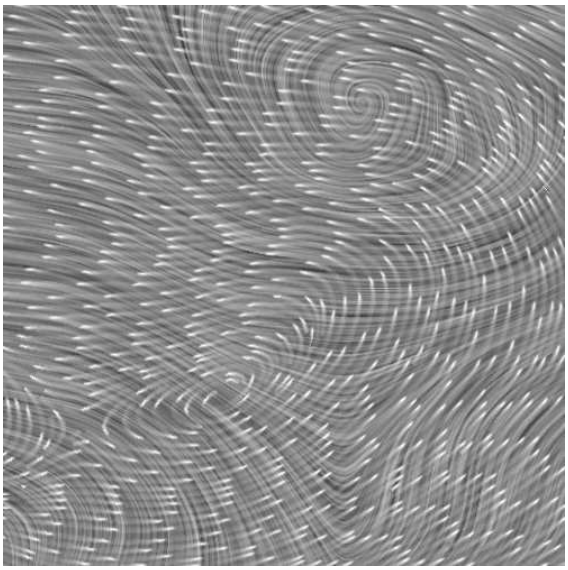

Figure 5: Glyph-texture mapped streamlines overlaid on a LIC texture mapped background

3.2 Embossing

In the overlay method, we primarily rely on luminance differences to distinguish the overlying glyph or line elements from the underlying texture image. Embossing is an alternative technique that can be employed to distinguish an overlaid image from an underlying image [9]. In this method, each element of the overlaying image is given a distinct 3D visual appearance, in order to enable the elements to perceptually group preferentially with each other and at the same time jointly segregate from the background.

Embossing algorithms simulate a standard lighting equation with a single point light source. While this method is highly effective in many situations, artifacts can arise when attempting to emboss vector fields, particularly when the vectors are oriented in the same direction as the light source. To sidestep this problem, we implemented the embossing using two different lights in the plane: one from a source directly above the image, and one from a source that is above

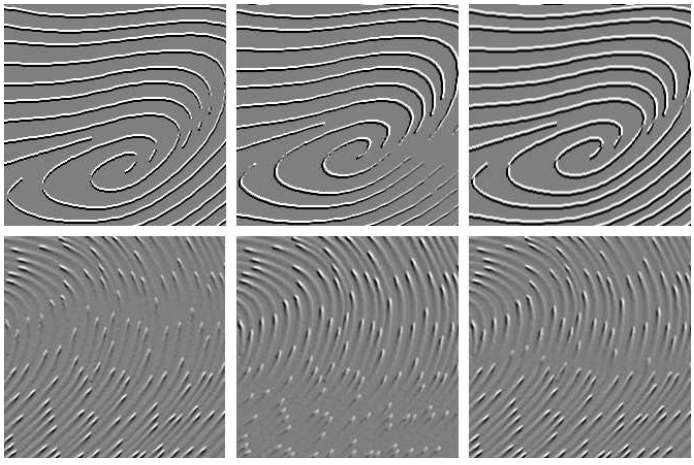

Figure 6: Embossing with different light source angles on streamlines (top row) and glyphs (bottom row). Left: Light source from directly above (90 degrees). Vectors vertically oriented aren't illuminated well. Middle: Light source from 45 degrees. In this case, the representation of the diagonally oriented vectors suffers. Right: Both light sources combined.

and to the right of the image, i.e. at a 45 degree angle to the image. The combination of these directions gives the impression of a broad light coming from "above." This produces the visual effect of the embossed image being raised from the surface. We create the composited image on a pixel-by-pixel basis by sampling from the appropriate input image, depending on the orientation of the flow at each point (taking care to always sample from an image that was created using a light source direction that is not aligned with the vector field). Regions of transition are alpha blended between the two images (figure 6).

Where it is relatively straightforward to emboss streamlines and glyphs, dense textures typically do not contain a sufficient amount of empty space within the image in which to portray the result of the shading equation. Textures can be embossed by utilizing an algorithm that creates a sparse texture to which the embossing algorithm can then be applied (figure 7).

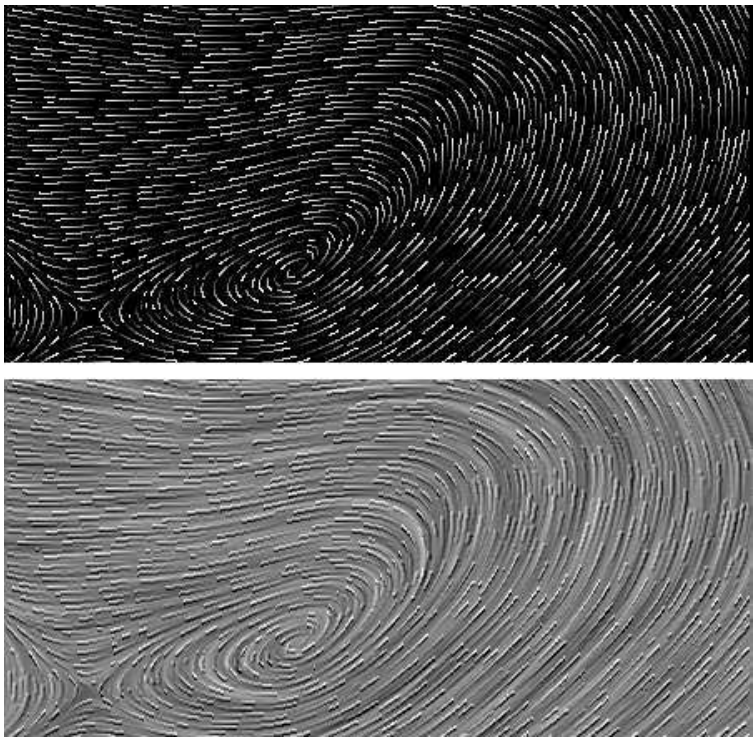

Figure 7: Embossing a texture. Top: A sparse texture in which the effects of an embossing algorithm can be perceived. Bottom: An embossed sparse texture combined with a LIC texture.

An embossed image can be overlaid on another image by adding the intensities in the two images on a pixel-by-pixel basis, and then subtracting the value that the background color takes in the embossed image. This is equivalent to increasing the intensity in the non-embossed image at the points where the intensity in the embossed image is above average, and decreasing the intensity in the non-embossed image at the points where the intensity in the embossed image is below average (figure 8). The embossing, in effect, gives a visual distinction of an applied 3D lighting equation and is visually separable from the non-embossed image.

As the initial results of layering a relatively sparse (glyph-like or streamline representation) of one vector field over a denser texture-based representation of the other vector field appear particularly promising, we use this approach to demonstrate the effective representation of two different, related vector fields in two scientific applications.

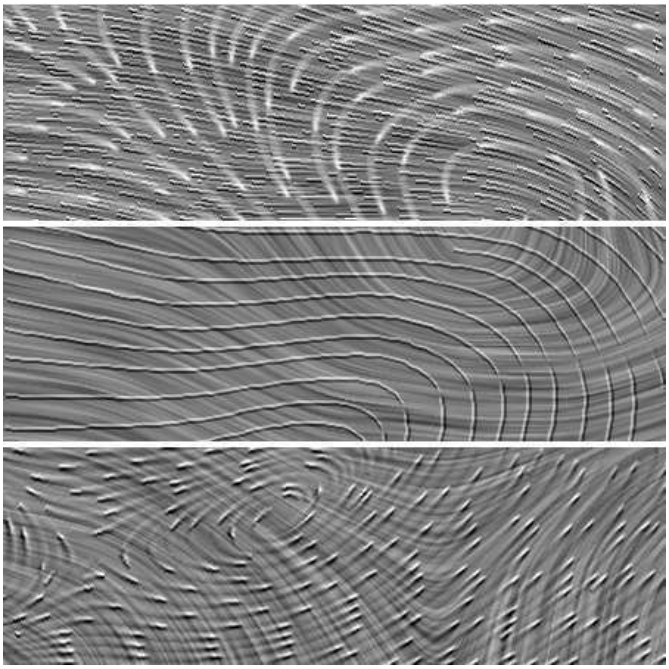

Figure 8: Distinguishing different fields by embossing. Top: embossed texture composited with glyphs. Middle: embossed streamlines composited with texture. Bottom: embossed glyphs composited with texture

4 Application 1: Experimental Turbulent Flow

We use the methods described to visualize data acquired from experimentally generated dual plane PIV experiments. Our goal is to further understand the relationship between the vorticity vector field, velocity vector field, and 2D and 3D swirl strength scalar distributions.

Understanding the coincidence of the velocity and vorticity fields is of interest to a number of investigators, particularly in conjunction with the visualization of vortex core locations. These visualizations allow for the analysis of several terms such as $(\vec{v} \times \vec{w})$, called the *Lamb* vector, and $(\vec{v} \cdot \vec{w})$ which is proportional to *helicity*, both of which have been suggested as possible descriptors of vortex tubes [6]. By visualizing multiple quantities, we are able to better develop theories about the *integrated* system, not just individual components of the data.

4.1 Swirl Strength

In an effort to understand and identify the subtle components of fluid dynamics, a number of vortex identification methods have been developed. Jeong and Hussain [4] indicated that the second invariant of the velocity gradient tensor, λ_2, is a quantity that measures the dominance of vorticity over strain and proposed that it could be used as a criterion to identify vortices. Zhou et al. [13] suggested the use of the imaginary part of the complex eigenvalue (λ_{ci}) of the velocity gradient tensor to visualize vortices. This value is referred as the local *swirl strength* of the vortex. In the calculations presented in this paper, we use the Zhou et al. definition.

A simplified version of swirl strength using a 2D velocity gradient can be computed to identify vortex cores. This quantity is referred to as the 2D swirl scalar field and is limited to identifying vortex cores that are oriented in a position normal to the sampling plane. Dual plane PIV is an extension of single plane PIV in which velocity components are measured in two planes simultaneously. This allows for all 3D velocity gradient measurements to be calculated. The

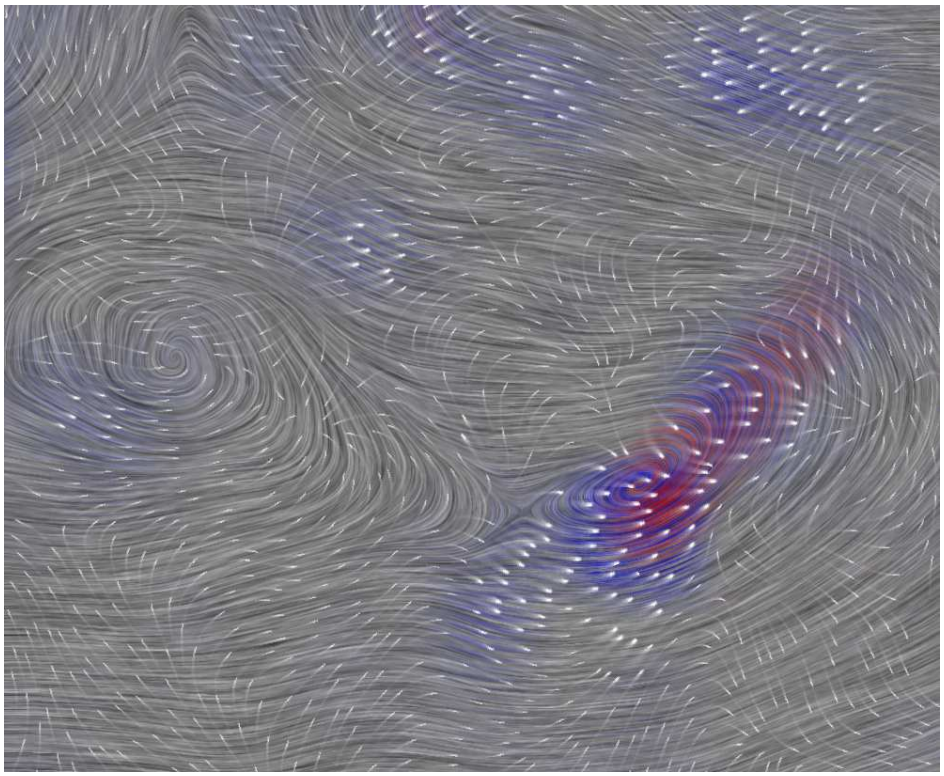

Figure 9: Visualization of multiple scalar and vector fields from a dual plane PIV experiment. The underlying LIC texture represents the velocity vector field. The field of glyphs represent the vorticity vector field. 2D swirl strength (red) and 3D swirl strength (blue) are represented in color. The combination of variables within a single image allows for the analysis of the contributions of each of the individual components to the potential of a vortex core.

corresponding 3D swirl scalar field is a measure of the existence of a vortex core in any orientation. The 2D and 3D swirl distributions are further discussed in conjunction with velocity and vorticity vector fields in the next section.

4.2 Vorticity, Velocity and Swirl Strength

We first analyze the in-plane velocity vector along with the 2D and 3D swirl fields. The velocity vector field is visualized using a LIC texture and the 2D and 3D swirl variables are encoded in color using a technique that maps each color to alternating streamlines to avoid the ambiguity that occurs when colors are mixed [10]. The LIC texture serves as a method to convey the underlying vector field while simultaneously providing the means to distribute the color representing additional scalar fields.

The velocity vector field is obtained by subtracting the mean streamwise velocity from the in-plane velocity component. Thus, the locations of critical points are subject to the relative velocity of the observer and are not germane to the analysis in this example. Swirling streamlines in the vicinity of the area of high swirl strength will only occur in the vicinity of the particular vortex cores that convect at a rate similar to the mean streamwise velocity.

Analyzing the relationship between the 3D swirl and 2D swirl components leads to a valuable understanding the of the orientation of a vortex core. As 3D swirl is calculated using all gradient components, it can accurately measure the potential of a vortex core at any orientation to the referencing plane. The 2D swirl distribution only measures the swirl of a vortex core that is oriented orthogonal to the plane. Accordingly, 2D swirl is present only where there is also significant 3D swirl.

To develop an understanding of how the vorticity vector field contributes to the phenomenon of swirl strength and the potential for a vortex core, we *screen overlay* the velocity vector field LIC image with a glyph image representing the

vorticity vector field (figure 9). Using the result of this image, we are able to analyze the relationships between the velocity and vorticity vector fields in a unique way that lends insight to how these two components interrelate.

The thickness of the glyphs is defined to be directly proportional to the in-plane vorticity magnitude. The two vector fields reveal zones where velocity and vorticity are nearly perpendicular (lower left and lower right of figure 9) and nearly parallel (leftmost zone of 3D swirl). The region exhibiting strong 2D swirl also contains strong in-plane vorticity, as evidenced by thick glyphs, and additional 3D swirl, suggesting a vortex core that is inclined at a significant angle to the measurement plane. The remaining zones of 3D swirl that lack a prominent indication of 2D swirl represent cores whose vorticity is more closely aligned with the measurement plane. The glyphs give the predominant vorticity direction of the core.

The integrated visualization of these components allows for vorticity direction and magnitude to be correlated with the direction of a vortex core delineated by swirl strength. Effectively combining techniques for the visualization of multiple vector and scalar fields allows for a better understanding of the complicated interactions that occur between the vortices.

5 Application 2: Computational Physics

The modeling of magnetohydrodynamic light supersonic jets in the context of astrophysical galaxy clusters is an area of active research in the field of computational physics. In addition to the velocity field, physicists are concerned with the magnetic vector field advected by these supersonic jets and are interested in analyzing the relationship between both vector fields. Developing a deeper understanding of the relationship between the vector fields' topology, magnetic field strength, and corresponding velocity structures results in a greater understanding about how kinetic and magnetic energy distributions evolve in these systems and contributes to the explanation of radio emissions that can be physically observed.

5.1 Magnetic Induction

Given a magnetic field $\vec{B}$, and a vector field $\vec{v}$, changes in magnetic field can be calculated from the ideal magnetic induction equation:

$$\frac{\partial \vec{B}}{\partial t} = \nabla \times (\vec{v} \times \vec{B})$$

This equation describes how motions of a perfectly conducting fluid change the magnetic fields contained therein. By examining the magnitude of this vector, we examine correlations between increases in magnetic field strength and anticipated shear or compression regions in the velocity field. Simultaneous visualization of all components of the velocity field and the rate of change of the magnetic field strength enables us to locate regions of active field enhancement, distinguish newly-magnified fields from those advected along with the plasma, and identify velocity structures that generate enhanced fields.

5.2 Multi-variate Visualization

Through simultaneous visualization of the simulated velocity and magnetic fields, we have been able to identify several regions of magnetic field enhancement and their antecedent velocity structures. We first visualize the velocity field using a high-frequency LIC texture with the magnitude of the magnetic induction equation represented in color. Next, the streamlines of the magnetic vector field are applied using the embossing technique introduced in section 3.2. The magnitude of the magnetic field is visualized using the thickness of the texture. The result is shown in figure 10.

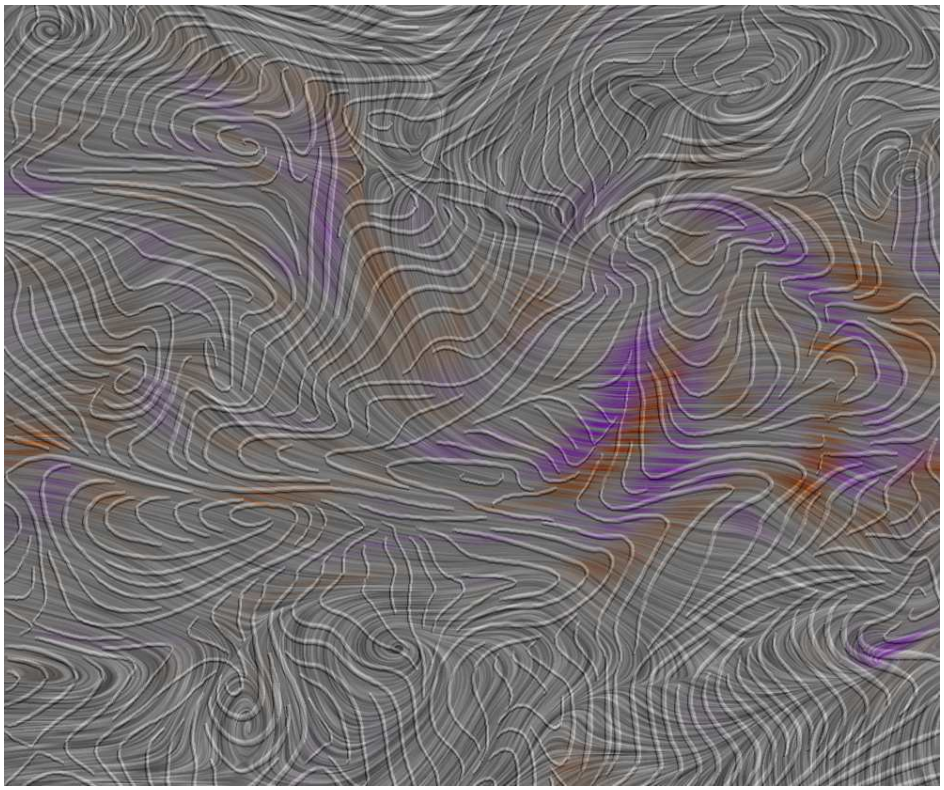

Figure 10: Visualization of multiple scalar and vector fields within a magnetohydrodynamic supersonic jet. The underlying LIC texture depicts the velocity vector field. The embossed streamlines represent the magnetic vector field. Purple (negative) and orange (positive) colors are used to represent the magnitude of the magnetic induction vector. The visualization of the vector and scalar fields in combination allows for advanced study of the correlation of variables within a magnetohydrodynamic supersonic jet.

Careful analysis of figure 10 reveals that there are regions of high magnetic field strength obviously correlated with particular velocity structures such as high-speed flows, flow compression, and shearing between flow structures. Areas in which there exist positive regions of magnetic induction ($\frac{\partial \vec{B}}{\partial t}$) indicate regions of magnetic field amplification. Regions of alignment of the magnetic vector field and the velocity field are a result of shear enhancement of the magnetic field. There are, however, additional magnetic enhancements with which the velocity field is not obviously causally connected. Moreover, there are many instances in which the magnetic field is unaligned or even orthogonal to the velocity field. This observation runs contrary to theoretical expectations, assuming shear is the dominant form of magnetic field amplification.

An understanding of the processes of magnetic field amplification and their relationship to flow velocity is important to astronomers since these magnetic structures are responsible for the observed radio emission characteristic of these systems. Through simulations and advanced visualization techniques, we expect to learn more about what observations of radio galaxies can tell us about the physics governing their evolution.

6 Conclusion and Future Work

Our main goal in this work has been to explore the development of visualization methods that can provide a deeper and more comprehensive understanding of the key interrelated features in coincident vector fields, augmented with the simultaneous display of related coincident scalar quantities. Our investigations have been driven by the needs of two important and diverse scientific applications: experimental investigations by aerospace engineers into the physics

of turbulence, and the computational modeling and simulation by astrophysicists of the behavior of supersonic jets in galactic clusters. In each of these application areas, we have demonstrated how our developed techniques facilitate the process of scientific inquiry. In future work, we plan to expand our investigations to consider a wider variety of texture patterns, beyond LIC. We are also considering employing techniques to explore the potential effectiveness of various alternative methods for simultaneously portraying multiple co-located vector and scalar fields in 3D.

References

[1] Brian Cabral and Leith (Casey) Leedom. Imaging vector fields using line integral convolution. In *Proceedings of SIGGRAPH 93*, pages 263–269. ACM, ACM Press / ACM SIGGRAPH, 1993.

[2] Ingrid Hotz, Louis Feng, Bernd Hamann, Kenneth Joy, and Boris Jeremic. Physically based methods for tensor field visualization. In *Proceedings of IEEE Visualization 2004*, pages 123–130, 2004.

[3] Victoria Interante. Illustrating surface shape in volume data via pricipal direction-driven 3d line integral convolution. In *Proceedings of SIGGRAPH 97*, pages 109–116. ACM, ACM Press / ACM SIGGRAPH, 1997.

[4] J. Jeong and F Hussain. On the identification of a vortex. *Journal of Fluid Mechanics*, 258:69–94, 1995.

[5] Robert M. Kirby, H. Marmanis, and David H. Laidlaw. Visualizing multivalued data from 2d incompressible flows using concepts from painting. In *Proceedings of IEEE Visualization 99*, pages 333–340, 1999.

[6] H. K. Moffatt. Magnetostatic equilibria and analogous euler flows of arbitrarily complex topology. i - fundamentals. *Journal of Fluid Mechanics*, 159:359–378, 1985.

[7] F. Taponecco and M. Alexa. Vector field visualization using markov random field texture synthesis. *Proceedings of Eurographics/IEEE TCVG Symposium on Data Visualization*, pages 195–202, 2003.

[8] Greg Turk and David Banks. Image-guided streamline placement. In *Proceedings of SIGGRAPH 96*, pages 453–460. ACM, ACM Press / ACM SIGGRAPH, 1996.

[9] Timothy Urness, Victoria Interrante, Ellen Longmire, Ivan Marusic, and Bharathram Ganapathisubramani. Techniques for visualizing multi-valued flow data. In *Eurographics/IEEE TCVG Symposium on Data Visualization*, 2004.

[10] Timothy Urness, Victoria Interrante, Ivan Marusic, Ellen Longmire, and Bharathram Ganapathisubramani. Effectively visualizing multi-valued flow data using color and texture. In *Proceedings of IEEE Visualization 2003*, pages 115–121, 2003.

[11] Jarke J. van Wijk. Spot noise — texture synthesis for data visualization. In *Proceedings of SIGGRAPH 91*, pages 309–318. ACM, ACM Press / ACM SIGGRAPH, 1991.

[12] C. Weigle, W. Emigh, G. Liu, R. Taylor, J. Enns, and C. Healey. Oriented sliver textures: A technique for local value estimation of multiple scalar fields. *Graphics Interface*, pages 163–170, 2000.

[13] J. Zhou, R. J. Adrian, R. J. Balachandar, and T. M. Kendall. Mechanisms for generating coherent packets of hairpin vortices in channel flow. *Journal of Fluid Mechanics*, 387:353–396, 1999.